Experimental Mechanics (2022) 62:943–952
https://doi.org/10.1007/s11340-022-00840-y

RESEARCH PAPER

Energy Absorption of Hourglass Shaped Lattice Metastructures

V. Gupta[1] · B. Bhattacharya[1] · S. Adhikari[1]

Received: 3 May 2021 / Accepted: 21 March 2022 / Published online: 11 April 2022

Abstract

Background The architected mechanical metastructures have garnered significant research attention for various engineering applications due to their remarkable mechanical properties and unique deformation behavior. The lattice-based microstructured materials have shown enhanced mechanical properties and the ability to control wave propagation, making them ideal for multifunctional applications.

Objective We report the family of lattice-based hourglass metastructures within the optimal design scope and its geometrical parameter selection. The lattice-based energy absorption performance and their damping characteristics have been classified based on different constitutive lattices.

Methods Herein, the uniaxial compressive response and lattice-based energy absorption capacity of a novel hybrid configuration, hourglass-shaped, consists of auxetic and honeycomb-based lattice, are systematically investigated through theoretical, finite element simulation and experimental methods. The proposed hourglass-shaped unit cell is a combination of two oppositely oriented coaxial domes that give more flexibility to control dynamic response and enhance lattice functionality passively. An additive manufacturing route has fabricated a series of hourglass-shaped lattice metastructures with nylon-based material.

Results It was found from the experimental data that the Ideal energy absorption efficiency parameter (E_i) is highest for the case of the auxetic-based hourglass with the increment of 22% and 35% than the solid shell and honeycomb lattice-based metastructure, respectively. The specific energy absorption parameters data have also been evaluated and compared with the numerical computational results.

Conclusion The combination of numerical simulation, additive layer manufacturing (3D printing), and experimental testing are implemented to quantitatively determine the lattice-based energy absorption properties and justify their evaluation. This study suggests the utilization of novel hourglass lattice-based metastructure for multifunctional engineering applications.

Keywords Hourglass cell · Metastructure · Auxetic lattice · Honeycomb lattice · Damping · Energy dissipation · Wave propagation

Introduction

The study of wave propagation in a periodic medium is an active field of research due to its diverse application in science and engineering. Periodic elastic media such as phononic crystals allow superior wave manipulation and control compared to conventional media [1, 2]. Thereby these advanced materials have opened up new challenges for designing acoustic and elastic devices [3]. These metamaterials are engineered with a bottom-up approach. They derive their fundamental properties from the geometry of their constitutive building blocks. In many cases, one or more constituent materials, building blocks, are structurally damped or dissipative in nature. The presence of damped building blocks results in temporal attenuation of the elastic waves as they freely progress through the periodic media. [4, 5]. It is in addition to the pass-band and stop-band of wave propagation.

Although many efforts have been devoted to studying the viscoelastic material-based damping, often used to form the matrix phase of phononic crystal composites [6], which has still its own advantages and disadvantages. Many researchers from the scientific community have put their

✉ B. Bhattacharya
bishakh@iitk.ac.in

[1] Department of Mechanical Engineering, Indian Institute of Technology, Kanpur, India

efforts into incorporating the damping from various alternatives. Some of them proposed particle-based damping for the phononic crystal. They found that the structure has emerged with excellent damping characteristics in medium and low frequencies regions. It contributes to extremely wide bandgap and low-frequency domain characteristics [7] on the dispersion diagrams. Others proposed dissipative dashpots for the bandgap broadening effects [8]. They investigated the effect of damping on the asymmetric wave transmission and found that the merging effect of dissipative dashpots can significantly enlarge the frequency bandwidths of asymmetric transmission regions.

The rapid development of additive layered manufacturing technology enables us the development of arbitrary complex geometries such as lattice-based topologies [9–13], woven topologies [14], hierarchical structures [15, 16], honeycomb structures, and foam-like metamaterials [17]. In turn, it provides an excellent opportunity to explore new mechanical metamaterials and metastructures based on unique geometries. During these developments, various designs are proposed to incorporate the dissipative and damping mechanisms. However, all these damping models have a limited scope of tunability due to the relatively simple geometry of building blocks. A broadband design on lattice-based metastructure requires novel unit cells. Hence, there is a need to design a unit metastructure with more customizable properties in terms of stiffness and damping. The lattice-based micro-structured materials have shown enhanced static properties and the ability to control wave propagation, making them ideal for multifunctional applications [18]. They opened up new areas of the tunable material property set.

It is observed from the existing literature that the dome-based lattice structures have rarely been explored in metastructure designs, particularly in the lattice-based damping as the repeated unit cell. Even though such systems have found an excellent potential to tune, the mechanical properties such as stiffness and Poisson's ratio [19]. We expand the design space of metastructure by integrating it with different lattice geometries to the hourglass shape. The system takes advantage of enhanced tunability of the hourglass metastructure with the combination of lattice-based damping. The shape of the hourglass structure is in itself an exciting design that contains a combination of two oppositely oriented coaxial domes. This configuration enables us to integrate standard lattices based on auxetic and regular honeycomb cells.

The hourglass lattice-based metastructures are proven highly customizable in terms of nonlinear stiffness [20]. However, little work has been done on their energy absorption capability and lattice-based damping performance. The topological variations in their constitutive cells provide a customizable stiffness and the range of system damping parameters.

This work evaluated, examined, and systematically categorized the lattice-based damping and energy absorption performance of homogeneous and nonhomogeneous hourglass metastructure unit cells. Experimental and numerical simulations have been presented, followed by the validations from published literature. Finite element analysis (FEA) of six hourglass metastructures was performed to analyze their dynamics in terms of frequency response and their lattice-based damping characteristics. An equivalent energy absorption model associated with the damping has been presented for quasi-static testing performed on six different hourglass lattice-based metastructures. This comprehensive study has also explored the effect of relative densities and lattice topology variations on the energy absorption efficiency parameters through various methods. The prospect of utilizing lattice-based metastructures for lightweight, multifunctional structures holds the potential for many engineering applications, such as automotive, aerospace, biomedical, and vibration isolation system for sensitive equipment.

Methodology

The proposed unit cell is modified as an hourglass-like shape with maximum section diameter *a* at the two ends and minimum section diameter *b* at the mid-horizontal plane, and it is symmetric about both the vertical planes that passes through the longitudinal axis of the hourglass. In Fig. 1, the d1 and d2 domes are interconnected by G1 continuous curved surface, which is formed through the revolute transformation of cubic spline about its longitudinal axis. The optimal design avoids stress concentration at connecting surfaces. Figure 1 schematically represents the hourglass-shaped lattice

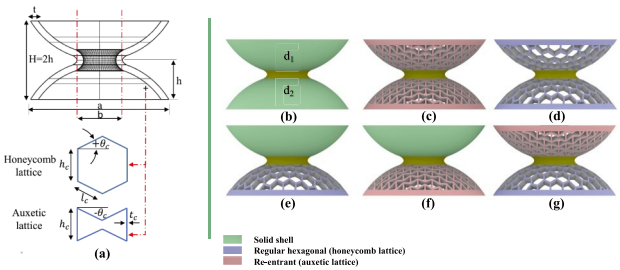

Fig. 1 Proposed hourglass shaped lattice metastructures, a combination of two domes d1 and d2 joined by G1 spline surface to avoid stress concentration **(b, c, d)** named as homogeneous (with d1 and d2 domes having lattice symmetry) and **(e, f, g)** non-homogeneous (with d1 and d2 domes having unsymmetrical lattices) categories. **(a)** Schematic of hourglass shape with standard lattices. Homogeneous: **(b)** hourglass as a solid shell (H:SS), **(c)** with regular honeycomb lattices (H:HH), **(d)** with auxetic lattices (H:AA). Non-homogeneous: **(e)** combination of regular honeycomb lattice with solid shell (NH:HS), **(f)** combination of auxetic lattices with solid shell (NH:AS), **(g)** combination of regular honeycomb with auxetic lattices (NH:HA)

metastructure which consists of combinations of two lattice based domes shown in different color schemes for the ease of understanding. Here, the sphere radius of d_1 and d_2 domes are 50 mm with the base radius a is 42 mm, H is the free height (undeformed) of the hourglass metastructure sample is equal to twice of h, i.e. height of a single dome, is 48 mm. Shell thickness t is taken 4 mm in radial direction of the domes. The constitutive cell parameters such as included cell angle θ_c (in the case of auxetic cells, it is re-entrant negative angle), cell lengths l_c, h_c and cell thickness t_c, is taken ±35°, 10 mm each and 1 mm respectively. The ratio of outer a and inner b base radius is r, a constant for all sample as shown in the Fig. 1(a). Two cellular lattice topologies are considered based on auxetic (re-entrant angle) and regular honeycomb. We have divided the hourglass metastructure into two classes for a comprehensive study: homogeneous (lattice symmetry between d1 and d2 domes) and non-homogeneous (unsymmetrical lattices between d1 and d2) as shown in Fig. 1(b-g) and the response of different samples have been observed.

The auxetic lattices are particularly favorable for adapting their shape as perfect domes because they exhibit an attractive negative Poisson's ratio property. Such deformation allows them to form a dome-shaped double curvature known as synclastic, which is not found in conventional hexagonal lattices. Moreover, 3D printing has emerged as a powerful and innovative additive layered manufacturing technology for developing such lattice-based complex metastructure designs. Therefore, we have modeled and printed six different classes of lattice-based hourglass metastructure. Their comparative energy absorption performance has been studied using quasi-static testing and the numerical simulation performed through the FEA software Ansys. The results are validated with the dynamic testing performed in published literature [20] in which dynamic characteristics such as frequency response of lattice-based hourglass metastructures have been explored with the help of laser Doppler vibrometer (LDV). A *non-contact laser Doppler vibrometer* is an interferometer-type device that replaces the physical placement of an accelerometer at a particular location of interest. It is based on the principle of detection of Doppler shift of the laser light scattered from the vibrating surface. The main component of LDV is the controller that establishes the communication link with the analyzer, where data acquisition (DAQ system) and signal processing take place to process the FFT signals. The exciter mechanism may be the separate component that is governed by the controller. The reported study presents displacement transmissibility test carried out using base excitation (pseudo-random signal with the resolution of 1600 FFT lines) of hourglass sample sandwiched between the top and bottom plate. The excitation was performed by the LDS-electrodynamic shaker (V780). The damping values for each sample have been evaluated experimentally using the half-power bandwidth method. The present study also validates the published damping values with the equivalent energy absorption metrics with the help of quasi-static testing and simulation results.

Material and Fabrication

Materials The flexible nylon based 3D printing material PCTPE (plasticized co-polyamide thermoplastic elastomer) supplied by Taulman 3D is used to additive layer manufacturing for developing all six hourglass based lattice metastructures as the testing samples. This study considers PCTPE as linearly elastic, homogeneous, isotropic material. The constitutive law involve three independent parameters i.e. Young's modulus, E, Poisson's ratio, ν, and shear modulus, G. The mechanical properties of PCTPE material are characterized by a Young's modulus of $E = 75$ Mpa, Poisson's ratio $\nu = 0.28$, and density $\rho = 0.96$ gm/cm^3. The flexibility of constitutive material ensures the appropriate functionality of lattice topologies under the applied loading conditions (see Table 1).

Fabrication using 3D printing The computer aided designs of the metastrcutures have been imported as stereolithography (STL) file using Ultimaker 3.0 Extended multi-material 3D printer and the slicing is performed on Cura 14.8. The developed metastructure samples are printed as a single body with d1 and d2 domes joined by a smooth spline surface to avoid stress concentration during loading-unloading processes. The modelling of homogeneous and non-homogeneous samples constitutes symmetrical and unsymmetrical lattice domes respectively. The standard lattices such as regular hexagonal based honeycomb and re-entrant based auxetic have been adopted for the comparative study with the solid shell geometry. The spherical radius of d1 and d2 domes are 50 mm, dome height (h) is 24 mm (makes the undeformed height of hourglass $H = 48$ mm), radial thickness 4 mm and the base radius is 42 mm. The thickness of the lattice beam kept 1 mm. The 3D printing parameters such as slicing resolution kept 0.15 mm layer thickness with 100% infill density and triangular infill pattern. While performing additive layered manufacturing, the necessary rectilinear and zig-zag supports (minimum 45° overhang angle) were used to prevent the dome from collapsing (the detailed parameters are shown in Table 2). The support pattern used for honeycomb lattices is gyroid type, which is found to be easy to remove while for

Table 1 Mechanical properties of the 3D printing materials

S.N	Mechanical properties	Values
1	Young's modulus of elasticity (E)	PCTPE: 75 mpa (hourglass)
2	Poisson's ratio	0.28
3	Density	PCTPE: 0.96 gm/cm^3

Table 2 A detailed 3D printing specifications used while developing the hourglass samples

S.N	3D printing specifications	Values
1	Material	PCTPE (hourglass) (2.85 mm nominal dia)
2	Layer height thickness	0.15 mm
3	Infill density	100 %
4	Infill pattern	Triangular
5	Printing bed temperature	235℃
6	Build plate temperature	84℃
7	Printing speed	60 mm/s
8	Support line distance, infill layer support line distance	2.3mm (both)
9	Support pattern	Zig-zag (auxetic and solid shell), gyroid (honeycomb lattice)
10	Support placement	Support overhang angle 45°
11	Support density	15 %
12	Build plate adhesion type	Brim, raft

others zig-zag type support pattern is found to be suitable. Within the limitation of 3D printing technology, the layer orientation is found to influence the mechanical properties of the material. Therefore, all the samples are printed with the same orientation on the build platform (see Fig. 2).

Experimental Study

Measurements/quasi-static testing

Quasi-static loading-unloading testing of six hourglass samples was conducted in universal testing machine Instron-1195 equipped with a ±2kN load cell, as shown in Fig. 3. The crosshead speed were set in displacement control mode at a strain rate 0.5 mm/min (quasi-static strain rate is less than $0.01s^{-1}$) in accordance with ASTM D3574-05, to accurately identify the naturally arising transition points [21]. The displacement control mechanism is set to apply compression loading up to the maximum load and then unloading is done with the same controlling parameters. The hysteresis loss with the retrieval of its original state was observed while unloading the sample, as shown in Fig. 5. It signifies the energy absorption in the loading-unloading process is significantly dependent on the lattice geometry. All measurements were conducted in similar conditions, where the samples were placed on a rigid platform and compressed with

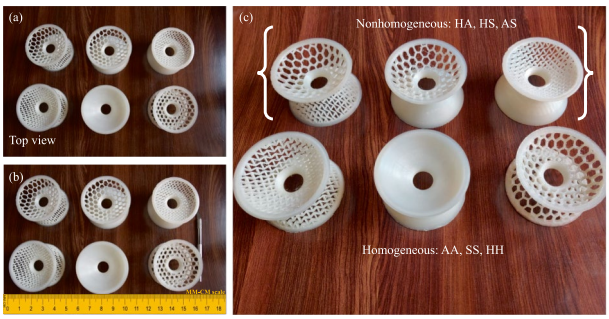

Fig. 2 3D printed samples using Additive manufacturing: (**a**) Finished 3D printed hourglass shaped metastrcuture (auxetic lattice based) with brim and supports. (**b**) Shown with the Length-scale indicator (MM-CM scale), after removal of all supports with the help of precision knife, (**c**) a well finished non-homogeneous hourglass shaped lattice metastructure sample with all functionally active lattices

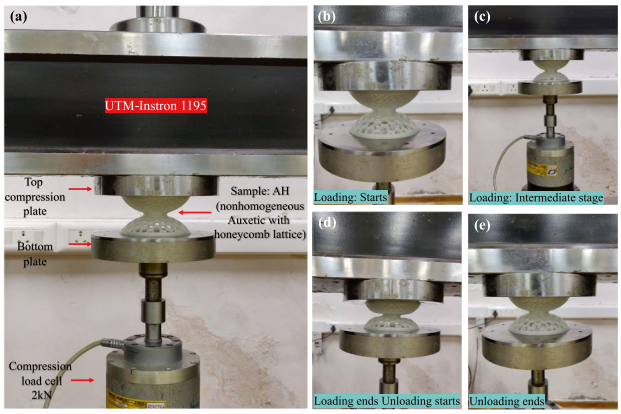

Fig. 3 Testing setup for quasi-static loading-unloading condition performed in universal testing machine Instron-1195 equipped with a 2kN load cell. (**a**) Nonhomogeneous 3D printed sample (NH:HA) is compressed between the top and bottom compression plate under displacement control mode at a strain rate 0.5 mm/min (**b**) Sample: Nonhomogeneous Auxetic with Honeycomb (NH:HA), loading begins under the displacement control environment with the measured loading-unloading range 0-125 N (**c**), (**d**), (**e**) shows the different compression stages. (**d**) is the maximum load attained 125 N, before the unloading begins. Similarly, all hourglass lattice samples were loaded till the peak load and then unloaded to initial stage, with the same strain rate

Table 3 Calculated energy dissipation parameters over the closed loop under the loading-unloading process in quasi-static testing. The SEA ψ, and efficiency parameters E_i, for homogeneous and non-homogeneous 3D printed hourglass lattice based metastructure

Loss parameter	AA	HH	SS	HA	AS	HS
A_h (in N-mm)	364.15	76.31	1.5×10^3	291.62	1.6×10^2	111.51
E_i, Ideal energy absorption efficiency parameter	0.210	0.155	0.172	0.211	0.171	0.154
ψ, Specific energy absorption (in J/gm)	0.052	0.014	0.109	0.047	0.015	0.012

circular shape compression plate. The permanent deformation was recorded using digital vernier calliper to make sure of any sample failure. The nonlinear curve with downward concave load deflection profiles were observed for all the samples and the enclosed area which determines the absolute energy absorption is found to be varying with lattice geometry, homogeneous and nonhomogeneous categorization and with solid shell metastructure.

Energy absorption of lattice based hourglass metastructures

The energy absorption of lattice based metastructures is defined as the area under the load-deflection curve. Various analytical metrics are available to evaluate the energy absorption performance of these kind of metastructures under the quasi-static and dynamic loading conditions. The most basic of these metrics is the Ideal absorbed enegry parameter, E_i and Specific energy absorption (SEA) ,ψ is well established through the literatures [22–25]. The E_i is also popularly known as Ideal energy absorption efficiency parameter, is defined as the ratio of absorbed energy by a real lattice metastrcuture upto to stress σ and strain ϵ to the energy absorbed by ideal absorber, i.e. under constant stress, up to the same strain level, and E_i can be expressed by

$$E_i = \frac{\int_0^{\epsilon_i} \sigma(\epsilon) d\epsilon}{\sigma \epsilon_i} \tag{1}$$

The definition of SEA is absorbed energy per unit mass, and it is calculated by

$$\psi = \frac{\int_0^{\epsilon_i} \sigma(\epsilon) d\epsilon}{\rho_\tau \rho} \tag{2}$$

where σ is the stress of the hourglass lattice metastructures (MPa), ϵ is the strain of the structure, and ρ_τ is the relative density of the lattice structures is a dimensionless number. It signifies the relative densities of hourglass samples, evaluated as the ratio with cell lattice to without cell lattice configuration i.e., solid shell. Effectively, it becomes mass ratio of hourglass with cells to without cells (solid shell hourglass) under the same volume i.e., all samples are considered with same shape and size. ρ is the density of the PCTPE, gcm^{-3}. For the evaluation of the energy absorption per unit volume, $\int_0^{\epsilon} \sigma(\epsilon) d\epsilon$, it is the ratio of enclosed area A_h, under the loading-unloading curves which represents the energy absorption of lattice sample (strain, ϵ_i upto the loading limit i) to the measured volume of the sample. The energy absorption performance indicators, E_i and ψ calculated separately for each sample are shown in Table 3 and evaluated in continuous domain with respect to strain percentage discussed in the later section. In the calculation of the energy efficiency parameter (E_i) , the energy absorption is considered using the enclosed shaded area A_h, under the loading-unloading curve on load-deflection plots obtained through the testing of the sample. Here, no stress-strain values have been considered separately because the denominator cancels out the per unit volume term of the numerator. On the other hand, the same energy value as above has been used for calculating specific energy absorption parameters (SEA), but it is now divided by volume. We used an equivalent diameter of a cylinder with the same volume of hourglass under consideration, which is treated as the mean diameter of the hourglass. The minimum diameter of the hourglass corresponds to the narrow region which lies in the middle plane has not considered because it over estimates the energy absorption value and its consideration is justified for the design point of view. On the other hand the maximum diameter lies on the top and bottom plane is underestimates the energy value and can be evaluated easily. The volume equivalent diameter for the hourglass (d_V) is evaluated from a basic expression of equating volumes of the hourglass and cylindrical shell is given by

$$V = \frac{\pi}{4} H_c [d_V^2 - d_i^2] \tag{3}$$

Here, V is the volume of each hourglass sample is obtained exactly through the numerical simulation model, d_i and d_V is inner and outer diameter of cylindrical shell. The inner dia. d_i can be expressed in terms of d_V using same thickness value t, of the hourglass sample. Treating free height H_c, of the cylinder shell is same as the height of hourglass shell H.

Finite Element Model

To determine the dynamic properties and frequency response of the numerical models, modal and harmonic analysis was performed in Ansys 18.1, as shown in Fig. 4. The analysis were carried out using mechanical APDL (ansys parametric design language) solver using tetrahedral mesh (relevance 68, fine sizing) with quadratic element order, the number of nodes and elements as 19564 and 8375 respectively for all the six samples. The subspace based algorithm is found suitable to extract modes for such a complex geometry and the mode superposition method is adopted for obtaining the harmonic responses. The generated frequency response functions (FRFs) captured a frequency range 0-500 Hz and comprised 1600 spectral lines, resulting in a frequency resolution of 0.3 Hz per data points, which equals the resolution obtained from dynamic experimental testing. The PCTPE material nonlinear effect with damping 0.1 has been considered with the flexible stiffness behavior for hourglass model and rigid stiffness for attached aluminium dead mass (200 gms).

To realize the actual testing conditions the base rib of hourglass is provided a zero displacement constraint to z-axis (hourglass axis) under displacement boundary condition. The face to face connection with slider tolerance 0.2 mm were established between attached mass and hourglass rib, allowing the remote displacement in z direction, as shown in Fig. 4.

Firstly, a modal analysis carried out for first 10 modes of all samples and extracted the frequency of deformation mode lies along its longitudinal axis. This gives a rough idea for considering the frequency domain for FRFs for each sample whether it is under failure limit or not.

A comparative study carried out between all the FRFs obtained and using the 'half power bandwidth method' around each peaks, damping for each sample has been calculated and shown in Table 5. The highest damping is observed in the case of homogeneous auxetic lattice based hourglass with the damping ratio $\zeta = 0.208$, followed by non-homogeneous hourglass based on solid shell and auxetic lattices with $\zeta = 0.166$, non-homogeneous based on solid shell with $\zeta = 0.141$, homogeneous hourglass of solid shell with honeycomb lattices with $\zeta = 0.12$, and non-homogeneous hourglass based on auxetic and honeycomb lattices with $\zeta = 0.1$. The 47% increment in ζ value is observed in auxetic lattice based hourglass metastructure than the solid shell hourglass and approx two times increment in damping is observed than the honeycomb lattice.

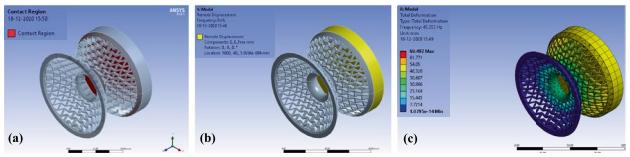

Fig. 4 Numerical simulation performed through finite element analysis (**a**) defining contact region between dead aluminium mass and PCTPE based hourglass model (**b**) applying remote displacement to z-axis (longitudinal axis) only and fix other constraints to zero, the average nodal displacement of all the nodes on the yellow faces in the X,Y coordinate direction is zero. (**c**) modal frequencies determination through the subspace algorithm

Results and Discussion

Quasi-static Testing

Quasi-static loading-unloading testing of six hourglass samples was conducted in universal testing machine Instron-1195 equipped with a ±2kN load cell, as shown in Fig. 3. Load-deflection profiles were shown in the Fig. 5, for three homogeneous (H:AA, H:HH, H:SS) and non-homogeneous (NH:AA, NH:HA, NH:HS) 3D printed samples. The closed loop under load-deflection profile indicates the dissipated energy through the lattice functional motion over one loading-unloading cycle. The calculated energy has been shown in Joules for load-deflection curves and Joules per unit volumes for σ-ϵ curve Table 3.

A comparative Ideal energy absorption efficiency parameter E_i, and specific energy absorption ψ, values are evaluated for each sample as shown in Table 3 for analysing its energy absorption and damping behaviour. The highest E_i is observed in the case of combinations of auxetic lattice based hourglass with the same auxetic lattice, honeycomb lattice and solid shell are E_i values 0.211, 0.2, 0.171 respectively.

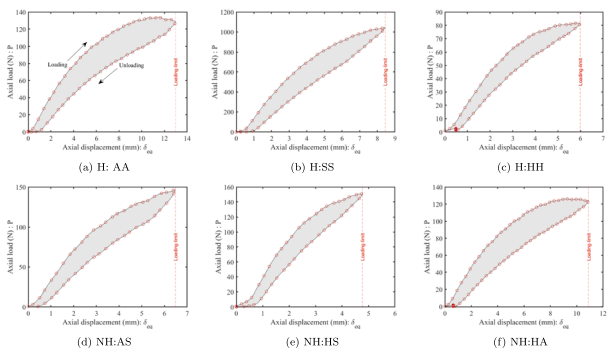

Fig. 5 The comparitive load-deflection curves obtained under the loading-unloading test in quasi-static strain rate (0.5 mm/min) condition, for six different lattice based hourglass structures. The comparison of static performance is obtained through experiments (tested in UTM with 2kN Load-cell) and analytical computations. The displacement control mechanism is set up to 35 % compression from the initial height of the sample. (**a**) Homogeneous auxetic (**b**) homogeneous solid shell hourglass (**c**) homogeneous regular honeycomb (**d**) non-homogeneous solid shell with auxetic (**e**) nonhomogeneous solid shell with honeycomb **(e)** nonhomogeneous auxetic lattice with honeycomb

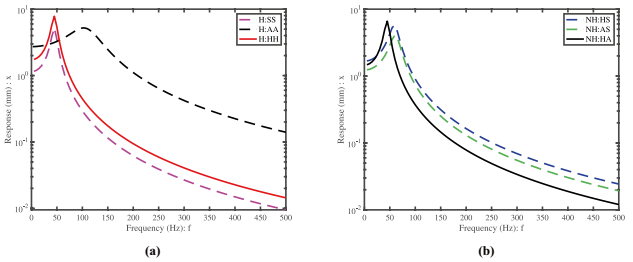

Fig. 6 Frequency response plots are obtained through the numerical simulation performed using finite element analysis software Ansys. The Harmonic excitation given to the base rib of the hourglass models and the generated FRFs were captured in a frequency range of 0-500 Hz. (**a**) Homogeneous hourglass metastructures (H:AA, H:SS, H:HH) (**b**) nonhomogeneous hourglass metastructures (NH:HS, NH:AS, NH: HA)

The 22% increment in E_i values is observed in auxetic lattice based hourglass metastructure than the solid shell hourglass and approx 35% increment is observed than the honeycomb lattice. Similarly, the specific energy absorption parameters are calculated and discussed in later sections (see Fig. 6).

FEA Simulations

The damping ζ, values obtained from the transmissibility tests performed in laser Doppler vibrometer [20] as shown in the Table 4 and compared with the FE numerical simulation results shown in the Table 5.

The Half-power Bandwidth Method for Damping ζ Calculation for Each Hourglass Lattice Metastructure

Damping in mechanical systems may be represented in numerous formats, including the one that uses the width of the peak value of the frequency response function of the structure. This damping estimation method is commonly known as the half-power bandwidth method and has the advantage of simplicity in application [26, 27]. The most common forms are Q and ζ , where Q is the amplification or quality factor ζ is the viscous damping ratio or fraction of critical damping.

Table 4 Transmissibility experiments are performed in laser Doppler vibrometer and obtained damping values ζ for the homogeneous and non-homogeneous category of hourglass lattice metastructure, using the half-power bandwidth method [20]

Hourglass sample (3D printed)	-3dB Points (Hz)		Q amplification factor	ζ
Homogeneous auxetic lattice	59.3	76.2	3.96	0.126
Homogeneous honeycomb lattice	61	76	5.61	0.089
Homogeneous solid shell	224	275.6	4.85	0.103
Non-homo. auxetic + solid	100	124.06	4.79	0.104
Non-homo. honeycomb + auxetic	68.7	85	4.7	0.105
Non-homo. honeycomb + solid	94.3	115.3	5.05	0.099

Table 5 The damping values ζ obtained from numerical simulations performed in FEA software ansys, for the homogeneous and non-homogeneous category of hourglass lattice metastructure, using the half-power bandwidth method

Hourglass sample (CAD model)	-3dB Points (Hz)		Q amplification factor	ζ
Homogeneous auxetic lattice	70	123	2.4	0.208
Homogeneous honeycomb	45	53	5	0.1
Homogeneous solid shell	40	55	3.54	0.141
Non-homo. auxetic + solid	35	55	3.01	0.166
Non-homo. honeycomb + auxetic	40.3	56.3	4.54	0.11
Non-homo. honeycomb + solid	38	58.6	4.16	0.12

A comparative study carried out between all the FRFs obtained and using the 'half power bandwidth method' around each peaks, damping for each sample has been calculated and shown in Table 5. The highest damping is observed in the case of homogeneous auxetic lattice based hourglass with the damping ratio $\zeta = 0.208$, followed by non-homogeneous hourglass based on solid shell and auxetic lattices with $\zeta = 0.166$, non-homogeneous based on solid shell with $\zeta = 0.141$, homogeneous hourglass of solid shell with honeycomb lattices with $\zeta = 0.12$, and non-homogeneous hourglass based on auxetic and honeycomb lattices with $\zeta = 0.1$. The 47% increment in ζ value is observed in auxetic lattice based hourglass metastructure than the solid shell hourglass and approx double increment is observed than the honeycomb lattice.

The frequency response obtained experimentally shows, the highest damping is observed in the case of homogeneous auxetic lattice metastructure with the damping ratio $\zeta = 0.126$, followed by non-homogeneous metastructure based on honeycomb and auxetic lattices with $\zeta = 0.1057$, non-homogeneous metastructure based on solid shell and auxetic lattices with $\zeta = 0.1042$, homogeneous metastructure of solid shell without lattices with $\zeta = 0.1033$, and non-homogeneous metastructure based on solid shell and honeycomb lattices with $\zeta = 0.0997$. The 21% increment in ζ value is observed in auxetic lattice based hourglass metastructure than the solid shell hourglass and approx 30% increment in damping is observed than the honeycomb lattice [20]. Here we define the quality factor or Q factor, which characterizes the system's bandwidth relative to the resonant frequency is expressed as:

$$Q = \frac{1}{2\zeta} \tag{4}$$

The Q value is equal to the peak transfer function magnitude for a single-degree-off freedom subjected to base excitation at its natural frequency. When the Q factor is low, the resonant peak becomes less significant, and the measurement of finding the change in the resonant frequency becomes difficult. The Q factor is also defined as the ratio of the energy stored in the system to the energy dissipated per cycle. When the Q factor is higher, the rate of energy loss is low, and the resonant frequency peak becomes sharper. The -3 dB points are also referred to as the half power points on the transfer magnitude curve expressed as:

$$2\zeta = \frac{(\omega_2 - \omega_1)}{\omega_n} = \Delta\omega/\omega_n \tag{5}$$

Where, ω_2 and ω_1 is the half-power points on the transfer magnitude curve, and $2\Delta\omega$ is called the half-power bandwidth (BW) as shown in Eq. 5, and ω_n is the natural frequency of the sample.

A Comparitive Energy Absorption Performance of Hourglass based Lattice Metastructures

Energy dissipation may be quantified in terms of damping parameters ζ, and further, it can be correlated with the non-dimensional energy absorption efficiency parameters obtained by the quasi-static testings. This study evaluates the damping ratio parameters using numerical simulations and validated with the ζ values obtained from the dynamic tests performed in laser Doppler vibrometer [20]. Moreover, all these data have been analysed under the same frame of the domain for a comparative analysis judiciously. It has been found the non-dimensional energy efficiency parameter follows the same trend with the damping ratio values obtained from the frequency response data obtained through the dynamic testing and the simulation one. From the Table 3 and Fig. 7, this has been found the homogeneous auxetic-based hourglass metastructure is more efficient in terms of energy absorption capacity compared to honeycomb lattice metastructure.

The energy absorption properties of hourglass based lattice metastructures obtained over the entire strain domain (in percentage), as shown in Fig. 8. With the high strength and maximum loading limit, the homogeneous solid shell enclosed area is maximum among the other 3D printed metastructures. Therefore the specific energy absorption of the homogeneous solid shell (H: SS) is highest among all the metastructures, and it is approximately doubled from homogeneous auxetic-based metastructure. It signifies, the homogeneous solid shell-based hourglass metastructures should

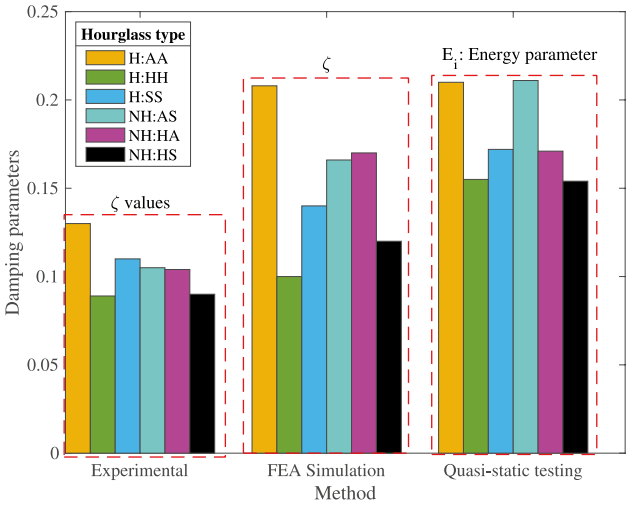

Fig. 7 A comparison of energy absorption parameters such as damping ratio, ζ and energy efficiency parameters E_i obtained through the dynamic testing performed in laser Doppler vibrometer, numerical simulation using finite element analysis, and the quasi-static tests done in universal testing machine respectively

be preferred in high energy absorption capacity in terms of weight optimization under the same maximum loading limit.

It is found from the experimental data; The homogeneous auxetic-based hourglass metastructure is most efficient in terms of ideal energy absorption parameter. It signifies these kinds of lattice metastructure are preferred under low

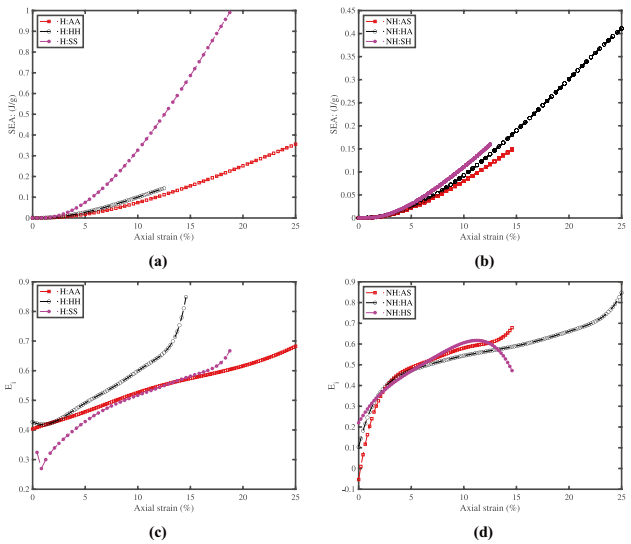

Fig. 8 The energy absorption properties of hourglass based lattice metastructures obtained over the entire strain domain (in percentage). The (**a,b**) specific energy absorption (SEA) and (**c,d**) energy efficiency parameters (E_i) are plotted for loading profile of stress-strain curve

stress-strain values where attaining maximum strength is not the constraint in the design problem. The auxetic-based metastructure is suitable as a building block damped mechanical metamaterial. They give tunable lattice-based damping, which is applicable for temporal attenuation of the elastic wave transmission as they freely propagate through periodic media.

The SEA and energy absorption plots are obtained over the entire strain domain (calculated in terms of percentage) through the quasi-static testing data. A generalized logic of the energy dissipation through the system equals the energy absorbed by the system subtracted by the energy rejected/returned from the system. Figure 8 shows that the energy-efficient parameter for loading is different for the homogeneous and non-homogeneous metastructure. A steep rise and then a fall has been observed in non-homogeneous honeycomb and lattice-based metastructure. On the other hand, a consistent rise has been observed for the homogeneous class of metastructure, specifically auxetic-based, that survives for larger strain values. Under loading conditions, energy is supplied efficiently for the homogeneous class of metastructure, especially honeycomb-based. Although, the net energy absorption is dependent upon the rejection efficiency as well. The net energy dissipation over the closed-loop has been evaluated and tabulated for all metastructure classes presented in Table 3.

Conclusions

This article systematically investigates the lattice-based energy absorption capacity of a novel hybrid configuration, hourglass-shaped, consisting of auxetic and honeycomb-based lattice, through theoretical, finite element simulation and experimental methods. The lattice-based damping capability of six categories of hourglass-shaped lattice metastructures with different lattices has been considered. The specific energy absorption and ideal energy absorption efficiency parameters measured from the quasi-static loading-unloading tests conducted on the universal testing machine (UTM) are reported. The following conclusions can be drawn from the study: The FRFs plots obtained from finite element analysis show that the damping factor (ζ) varies with the lattice geometry, which follows the similar trend as the energy efficiency parameters obtained from the testing of six 3D printed samples. The maximum energy absorption is observed in the homogeneous hourglass lattice metastructure with auxetic lattice followed by homogeneous honeycomb lattice-based metastructure. The homogeneous auxetic-based hourglass metastructure is efficient in terms of the ideal energy absorption parameter. It signifies these kinds of lattice metastructure are preferred under low stress-strain values where attaining maximum strength is not a constraint in the design problem.

It is observed that the relative densities of the lattice structure have a significant influence on energy absorption capacity and specific energy. This influence is more prevailing for similar stiffness-profile metastructures (like nonhomogeneous hourglass samples NH: AS and NH: HS) due to similar maximum strengths and loading conditions.

Specific energy absorption parameter for nonlattice-based hourglass metastructure has the highest value among all the metastructures. It signifies that the material damping becomes dominant over lattice-based damping due to its high mass-to-volume ratio when subjected to maximum loading conditions. The study also suggests that the homogeneous solid shell-based hourglass metastructures should be preferred in high energy absorption capacity in terms of weight optimization under the same maximum loading limit. The unique combination of high specific energy absorption with high energy efficiency parameters makes the lattice-based hourglass metastructure a promising candidate for the application for vibration isolation. This customizable lattice-based damping and tunable stiffness pave the way to make a suitable periodic unit cell for the tunable mechanical metamaterials.

Supporting Information

Supporting Information is available from the Wiley Online Library or from the author on request.

Acknowledgements VG and BB acknowledge the grants received from "Scheme for Promotion of Academic and research collaboration" (SPARC) and Ministry of Human Resource Development, Govt. of India (MHRD) through grant number MHRD /ME /2018544. SA acknowledges the support of UK-India Education and Research Initiative through grant number UKIERI/P1212.

Declarations

Conflicts of Interest The authors state that regarding the research and writing of the manuscript, there are no conflicts of interest and that all the authors consent to the content of the manuscript.

References

1. Liu Z, Zhang X, Mao Y, Zhu Y, Yang Z, Chan CT, Sheng P (2000) Locally resonant sonic materials. Science 289(5485):1734
2. Gdoutos E, Shapiro AA, Daraio C (2013) Thin and thermally stable periodic metastructures. Exp Mech 53(9):1735
3. Kushwaha MS, Halevi P, Dobrzynski L, Djafari-Rouhani B (1993) Acoustic band structure of periodic elastic composites. Phys Rev Lett 71(13):2022
4. Hussein MI (2009) Theory of damped Bloch waves in elastic media. Phys Rev B 80(21):212301
5. Mead D (1973) A general theory of harmonic wave propagation in linear periodic systems with multiple coupling. J Sound Vib 27(2):235

6. Mukherjee S, Lee EH (1975) Dispersion relations and mode shapes for waves in laminated viscoelastic composites by finite difference methods. Comput Struct 5(5–6):279
7. Wang C, Xiao W, Wu D, Wang S, Lin C, Luo Y, Xiao J, Yao K, Xu Z (2020) Study on bandgap characteristics of particle damping phononic crystal. Appl Acoust 166:107352
8. Alamri S, Li B, Mchugh G, Garafolo N, Tan K (2019) Dissipative diatomic acoustic metamaterials for broadband asymmetric elastic-wave transmission. J Sound Vib 451:120
9. Deshpande VS, Fleck NA, Ashby MF (2001) Effective properties of the octet-truss lattice material. J Mech Phys Solids 49(8):1747
10. Vigliotti A, Pasini D (2012) Stiffness and strength of tridimensional periodic lattices. Comput Methods Appl Mech Eng 229:27
11. Moongkhamklang P, Deshpande V, Wadley H (2010) The compressive and shear response of titanium matrix composite lattice structures. Acta Mater 58(8):2822
12. Geng LC, Ruan XL, Wu WW, Xia R, Fang DN (2019) Mechanical properties of selective laser sintering (SLS) additive manufactured chiral auxetic cylindrical stent. Exp Mech 59(6):913
13. Gupta V, Chattoraj A, Banarjee A, Bhattacharya B (2019) In: Active and passive smart structures and integrated systems XIII, vol 10967. International Society for Optics and Photonics, p 109671K
14. Erdeniz D, Levinson AJ, Sharp KW, Rowenhorst DJ, Fonda RW, Dunand DC (2015) Pack aluminization synthesis of superalloy 3D woven and 3D braided structures. Metall and Mater Trans A 46(1):426
15. Gatt R, Mizzi L, Azzopardi JI, Azzopardi KM, Attard D, Casha A, Briffa J, Grima JN (2015) Hierarchical auxetic mechanical metamaterials. Sci Rep 5:8395
16. Mousanezhad D, Babaee S, Ebrahimi H, Ghosh R, Hamouda AS, Bertoldi K, Vaziri A (2015) Hierarchical honeycomb auxetic metamaterials. Sci Rep 5(1):1
17. Ashby MF (2006) The properties of foams and lattices. Philosophical Transactions of the Royal Society A: Mathematical, Physical and Engineering Sciences 364(1838):15
18. Francesconi L, Baldi A, Dominguez G, Taylor M (2020) An investigation of the enhanced fatigue performance of low-porosity auxetic metamaterials. Exp Mech 60(1):93
19. Gupta V, Adhikari S, Bhattacharya B (2020) Locally resonant mechanical dome metastructures for bandgap estimation 11376:1137626
20. Gupta V, Adhikari S, Bhattacharya B (2020) Exploring the dynamics of hourglass shaped lattice metastructures. Sci Rep 10(1):1
21. Upadhyay K, Bhattacharyya A, Subhash G, Spearot DE (2019) Quasi-static and high strain rate simple shear characterization of soft polymers. Exp Mech 59(5):733
22. Gibson LJ, Ashby MF (1999) Cellular solids: structure and properties. Cambridge University Press
23. Ding R, Yao J, Du B, Zhao L, Guo Y (2020) Mechanical properties and energy absorption capability of arch lattice structures manufactured by selective laser melting. Adv Eng Mater 22(5):1901534
24. Koohbor B, Blourchian A, Uddin KZ, Youssef G (2020) Characterization of energy absorption and strain rate sensitivity of a novel elastomeric polyurea foam. Adv Eng Mater 2000797
25. Gan C, Gibson RF, Newaz GM (2004) Analytical/experimental investigation of energy absorption in grid-stiffened composite structures under transverse loading. Exp Mech 44(2):185
26. De Silva CW (2006) Vibration: fundamentals and practice. CRC Press
27. Chopra AK (2007) Dynamics of structures. Pearson Education India